Hindawi Publishing Corporation
International Journal of Photoenergy
Volume 2014, Article ID 786165, 8 pages
http://dx.doi.org/10.1155/2014/786165

*Research Article*

# The Photocatalytic Activity and Compact Layer Characteristics of $TiO_2$ Films Prepared Using Radio Frequency Magnetron Sputtering

**H. C. Chang,[1] H. H. Huang,[2] C. Y. Wu,[2] R. Q. Hsu,[1] and C. Y. Hsu[2]**

[1] *Department of Mechanical Engineering, National Chiao Tung University, 1001 University Road, Hsinchu 30010, Taiwan*
[2] *Department of Mechanical Engineering, Lunghwa University of Science and Technology, No. 300, Sec. 1, Wanshou Road, Guishan, Taoyuan 33306, Taiwan*

Correspondence should be addressed to C. Y. Hsu; cyhsu@mail.lhu.edu.tw

Received 7 March 2014; Revised 18 April 2014; Accepted 18 April 2014; Published 22 May 2014

Academic Editor: Ho Chang



$TiO_2$ compact layers are used in dye-sensitized solar cells (DSSCs) to prevent charge recombination between the electrolyte and the transparent conductive substrate (indium tin oxide, ITO; fluorine-doped tin oxide, FTO). Thin $TiO_2$ compact layers are deposited onto ITO/glass by means of radio frequency (rf) magnetron sputtering, using deposition parameters that ensure greater photocatalytic activity and increased DSSC conversion efficiency. The photoinduced decomposition of methylene blue (MB) and the photoinduced hydrophilicity of the $TiO_2$ thin films are also investigated. The photocatalytic performance characteristics for the deposition of $TiO_2$ films are improved by using the Grey-Taguchi method. The average transmittance in the visible region exceeds 85% for all samples. The XRD patterns of the $TiO_2$ films, for sol-gel with spin coating of porous $TiO_2$/$TiO_2$ compact/ITO/glass, show a good crystalline structure. In contrast, without the $TiO_2$ compact layer (only porous $TiO_2$), the peak intensity of the anatase (101) plane in the XRD patterns for the $TiO_2$ film has a lower value, which demonstrates inferior crystalline quality. With a $TiO_2$ compact layer to prevent charge recombination, a higher short-circuit current density is obtained. The DSSC with the FTO/glass and Pt counter electrode demonstrates the energy conversion efficiency increased.

## 1. Introduction

Dye-sensitized solar cells (DSSCs) have been extensively studied as a promising alternative to conventional solar cells that use a p-n junction because of their reasonable conversion efficiency, low cost, environmentally friendly components, use of a flexible cell design, and simple fabrication process, when compared to silicon solar cells [1]. DSSCs are the next-generation solar cells [2]. If low cost and highly efficient DSSCs can be developed, it will be an important new direction for the development of solar cells. A typical DSSC consists of dye molecules that act as sensitizers, a nanoporous metal oxide film ($TiO_2$ semiconductor material), a transparent conducting oxide (indium tin oxide, ITO), an electrolyte charge carrier, and a counter electrode (Pt or carbon) [3]. The dye and metal oxide, which are used for the sensitizer and the electrode, respectively, are important to the photoelectric conversion efficiency of DSSCs [4].

$TiO_2$ is one of the most popular photocatalytic materials, so it has many commercial applications, such as antibacterial applications, waste purification, self-cleaning, and sensors [5]. It is also used for photoelectrodes and in high performance DSSC applications because it has an adequate photoresponse and effective electron transport [6]. A high incident photon to current conversion efficiency is expected for $TiO_2$ films that have a better phase structure and crystallinity and a higher specific surface area [7]. The control of the $TiO_2$ nanostructures is very important for the photovoltaic performance of a DSSC [8]. In order to improve the conversion efficiency of DSSCs, several studies have focused on the structural design, material development, photovoltaic characterization, and analysis of the mechanism of $TiO_2$

Table 1: The factor and level settings for sputter deposition of $TiO_2$ compact layers.

| | | | | |
|---|---|---|---|---|
| Substrate | | Soda-lime glass, $20 \times 20 \times 1\,mm^3$ | | |
| Target | | $TiO_2$ (99.99% purity) | | |
| Gas | | Ar and $O_2$ (99.99% purity) | | |
| Base pressure | | $5.0 \times 10^{-6}$ torr | | |
| Substrate-to-target distance | | 80 mm | | |
| Substrate temperature | | Room temperature | | |
| Substrate rotate vertical axis | | 10 rpm | | |
| Symbol | Control factor | Level 1 | Level 2 | Level 3 |
| A | rf power (W) | 100 | 130 | 160 |
| B | Sputtering pressure (mtorr) | 3 | 5 | 7 |
| C | $O_2/(Ar + O_2)$ (%) | 10 | 30 | 50 |
| D | Deposition time (hr) | 2 | 3 | 4 |

nanoparticles [9]. Mesoporous $TiO_2$ is widely used as an electrode in DSSCs to produce a high surface area for the adsorption of a greater density of dye molecules, which produces a significant increase in the photocurrent [10]. However, the highly porous structure of the $TiO_2$ layer can cause an electrical shortage and recombination of the charge/electrons, which interferes with the unidirectional electron transport that takes place at the $TiO_2$ layer/dye molecule and ITO/$TiO_2$ layer interfaces [11]. This leakage by electronic back transfer leads to a decrease in cell efficiency. To avoid this problem, the primary method used to prevent recombination is the use of a $TiO_2$ compact layer (blocking layer) between the ITO and the porous $TiO_2$ layer [11]. This compact layer can be prepared using many growth techniques, such as sputter deposition, dip-coating, chemical vapor deposition, and spray pyrolysis.

This study determines the optical, structural, and surface properties of a $TiO_2$ compact layer that is grown by radio frequency (rf) magnetron sputtering on the ITO electrodes, as a function of the deposition parameters that ensure higher photocatalytic activity and greater DSSC conversion efficiency. The nanoporous $TiO_2$ upper layer is coated using the sol-gel process and calcination at 450°C. Moreover, the working electrode which is made of a dye-sensitized $TiO_2$ film that is immobilized onto a fluorine-doped tin oxide (FTO) substrate is also investigated.

The Taguchi method is a powerful tool for the design of high quality systems, which can be used to design low cost products, with improved quality [12]. To optimize the deposition process for $TiO_2$ photocatalytic films, a statistical analysis of the signal-to-noise ratio ($S/N$) is performed, using an analysis of variance (ANOVA). The optimal deposition parameters are obtained by analyzing the results for various experimental permutations [13, 14]. Table 1 shows the effect on the quality of the $TiO_2$ photocatalytic films of four deposition parameters at three levels: the rf power, the sputtering pressure, the Ar-$O_2$ ratio, and the deposition time. An $L_9$ ($3^4$, with four columns and nine rows) orthogonal array is used.

## 2. Experimental

The $TiO_2$ photocatalytic thin films (compact layer) were coated onto ITO/glass substrates (and FTO/glass), using rf magnetron sputtering. The reactive and sputtering gases were $O_2$ (purity: 99.99%) and Ar (purity: 99.99%), respectively. The commercially available, hot pressed, and sintered ceramic target $TiO_2$ had a diameter of 50.8 mm and 99.99% purity (Elecmat, USA).

Prior to coating, the target was presputtered for 15 min, in order to remove any contamination, and the substrates were ultrasonically cleaned and degreased in acetone, rinsed in deionised water, and subsequently dried with nitrogen gas. A vacuum, of base pressure $5.0 \times 10^{-6}$ Torr, was applied before deposition. The distance between the substrate and the target (80 mm) and the rotational speed of the substrate (10 rpm) were constant. By adjusting the experimental permutations, this study determined the effect of each deposition parameter on the deposition rate for $TiO_2$/ITO/glass, the methylene blue (MB) absorbance, the contact angle to a pure water droplet, the surface morphology, and the crystal structure.

The porous $TiO_2$ film (p-$TiO_2$) was coated onto the $TiO_2$ compact/ITO/glass (and $TiO_2$ compact/FTO/glass) using a mixture of $TiO_2$ powders (P-25, particle size: <25 nm, 99.7%) with the $TiO_2$ sol-gel component studied in [15]. The $TiO_2$ sol-gel was mixed with 0.3 g of commercially available Degussa P-25, to avoid any cracking of the film. The $TiO_2$ sol-gel was produced using spin coating and blade coating. The gels were predried for 15 min at 50°C and then sintered in a box furnace at 450°C (heating rate 10°C/min) for 30 min in air ambient, to produce the bare $TiO_2$ electrode used in this work to fabricate the DSSC. The porous $TiO_2$ films were immersed into the dye solution (0.4 mM N719 dye solution, Solaronix, Switzerland, Di-tetrabutylammonium cis-bis(isothiocyanato)bis(2, 2′-bipyridyl-4,4′-dicarboxylato)-ruthenium(II); chemical formula $C_{58}H_{86}N_8O_8RuS_2$; Mol Wt: 1188.55) complex for 24 h at room temperature.

Table 2: The experimental results and the $S/N$ ratios for the deposition rate, the contact angle, and the MB absorbance for the $TiO_2$ compact layer coatings (the experiments were repeated twice).

| Exp. | Factors | | | | Deposition rate (Å/min) | | $S/N$ (dB) | Water contact angle (degree) | | $S/N$ (dB) | MB absorbance | | $S/N$ (dB) |
|---|---|---|---|---|---|---|---|---|---|---|---|---|---|
| | $A$ | $B$ | $C$ | $D$ | $T1$ | $T2$ | | $T1$ | $T2$ | | $T1$ | $T2$ | |
| 1 | 1 | 1 | 1 | 1 | 3.35 | 3.00 | 9.9953 | 90.73 | 91.30 | −39.182 | 1.328 | 1.332 | −2.4770 |
| 2 | 1 | 2 | 2 | 2 | 2.73 | 3.04 | 9.1653 | 92.13 | 91.87 | −39.275 | 1.327 | 1.325 | −2.4508 |
| 3 | 1 | 3 | 3 | 3 | 2.19 | 2.23 | 6.8868 | 73.91 | 75.40 | −37.461 | 1.296 | 1.293 | −2.2420 |
| 4 | 2 | 1 | 2 | 3 | 4.85 | 4.97 | 13.8197 | 89.75 | 90.28 | −39.086 | 1.198 | 1.187 | −1.5292 |
| 5 | 2 | 2 | 3 | 1 | 4.35 | 3.95 | 12.3307 | 91.01 | 92.71 | −39.262 | 1.284 | 1.283 | −2.1679 |
| 6 | 2 | 3 | 1 | 2 | 4.84 | 4.76 | 13.6239 | 93.57 | 94.68 | −39.474 | 1.205 | 1.200 | −1.6017 |
| 7 | 3 | 1 | 3 | 2 | 6.38 | 6.11 | 15.9046 | 71.70 | 72.30 | −37.146 | 1.287 | 1.284 | −2.1814 |
| 8 | 3 | 2 | 1 | 3 | 7.48 | 7.25 | 17.3403 | 95.35 | 94.81 | −39.561 | 1.077 | 1.074 | −0.6322 |
| 9 | 3 | 3 | 2 | 1 | 4.73 | 4.82 | 13.5783 | 63.79 | 62.39 | −35.999 | 1.031 | 1.030 | −0.2609 |

Note: $A$ = rf power (W), $B$ = process pressure (Pa), $C = O_2/(Ar + O_2)$ flow rate ratio (%), and $D$ = deposition time (hr).

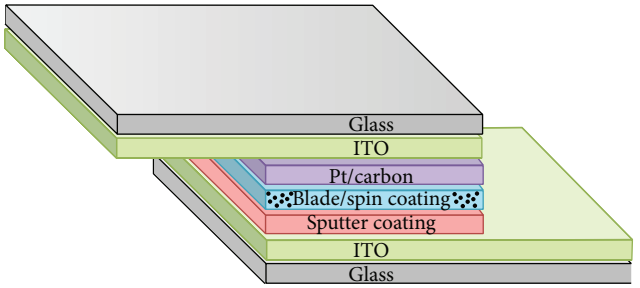


Figure 1: A schematic diagram of a DSSC with an rf-sputtered $TiO_2$ compact layer/ITO/glass on the ITO electrode.

The Pt counter electrode was coated onto ITO/glass (and FTO/glass) substrates using DC sputtering with pure Ar gas and a DC power of 30 W. The dye-adsorbed $TiO_2$ working electrode and the counter electrode were assembled into a sandwich-type cell and sealed with a hot-melt sealant. Figure 1 shows a schematic diagram of a DSSC with an rf-sputtered $TiO_2$ compact layer/ITO/glass on the ITO electrode. In order to prevent the leakage by electron transfer to the liquid electrolyte, dense $TiO_2$ passivating layers were used.

The phase identification of the particles produced using various deposition parameters was performed by X-ray diffraction (Rigaku-2000 spectrometer), using Cu-K$\alpha$ radiation (40 kV, 30 mA, and $\lambda = 0.1541$ nm). The photoinduced hydrophilicity of the $TiO_2$ thin films was evaluated by measurement of the contact angle to pure water, using a contact angle meter (FACE CAVP150) that is accurate to less than 1°. A black light (UVP UVL-225D) lamp with a principal wavelength of 365 nm (1.5 mW/cm$^2$ at the film surface) was the UV light source. The decomposition of MB aqueous solution (10 $\mu$M) was photocatalyzed. An UV-Vis-NIR spectrometer (Jasco V-670) was used to measure the absorption spectra of the MB solution as a function of the UV irradiation time. The film thickness was measured, using a surface profilometer ($\alpha$-step, AMBIOS XP-1). The surface morphology was analyzed using a field emission scanning electron microscope (FESEM, JEOL JSM-6500F). The crystal structure of the films was characterized by X-ray diffraction (Rigaku-2000 spectrometer), using Cu-K$\alpha$ radiation (40 kV, 30 mA, and $\lambda = 0.1541$ nm), with a grazing incidence angle of 1°. The scanning rate was 5°/min.

The power used to test the prepared DSSC was a 150 W Xe lamp, which simulates sunlight (AM 1.5). Before the test, the distance between the light source and the sample was adjusted to allow a light source density of 100 mW/cm$^2$. The cell performance parameters, including the short-circuit current density ($J_{sc}$), the open-circuit voltage ($V_{oc}$), the fill factor (FF), and the photoelectronic conversion efficiency ($\eta(\%) = J_{sc} \times V_{oc} \times \text{FF}/\text{total incident energy} \times 100$), were measured and calculated using the $J$-$V$ characteristics of DSSC.

## 3. Results and Discussion

*3.1. The Photocatalytic Activity of the $TiO_2$ Compact Films.* The $TiO_2$ compact films were deposited onto ITO soda-lime glass substrates. The optimization of the parameter settings involved comparing the signal-noise ($S/N$) ratios, using the Taguchi method. In order to optimize the $TiO_2$ compact films deposition parameters, the water contact angle and the MB absorbance had the smaller the better characteristics and the deposition rate had the larger the better characteristics. The respective $S/N$ ratios for the smaller the better characteristic and the larger the better characteristic are expressed as follows (Taguchi et al. [13]):

$$\left(\frac{S}{N}\right)_S = -10 \log \frac{1}{n} \sum_{i=1}^{n} y_i^2$$
$$\left(\frac{S}{N}\right)_L = -10 \log \frac{1}{n} \sum_{i=1}^{n} \frac{1}{y_i^2}, \quad (1)$$

where $n$ is the number of iterations for the experiment and $y_i$ is the $i$th average value of the characteristic measured.

Table 3: The ANOVA results for the deposition rate, the water contact angle, and the MB absorbance.

| Factor | Degree of freedom | Sum of square | Variance | Contribution ($P$ %) |
|---|---|---|---|---|
| Deposition rate (Å/min) | | | | |
| $A$ | 2 | 74.4166 | 37.2083 | 84.45 |
| $B$ | 2 | 6.1132 | 3.0566 | 6.93 |
| $C$ | 2 | 6.1644 | 3.0822 | 7.00 |
| $D$ | 2 | 1.4211 | 0.7106 | 1.62 |
| Total | 8 | 88.1153 | | 100 |
| Water contact angle (degree) | | | | |
| $A$ | 2 | 4.4559 | 2.22793 | 33.68 |
| $B$ | 2 | 4.4483 | 2.22417 | 33.62 |
| $C$ | 2 | 3.7790 | 1.88950 | 28.56 |
| $D$ | 2 | 0.5472 | 0.27359 | 4.14 |
| Total | 8 | 13.2304 | | 100 |
| MB absorbance | | | | |
| $A$ | 2 | 2.80223 | 1.40111 | 54.36 |
| $B$ | 2 | 0.72560 | 0.36280 | 14.07 |
| $C$ | 2 | 1.03120 | 0.51560 | 20.00 |
| $D$ | 2 | 0.59634 | 0.29817 | 11.57 |
| Total | 8 | 5.15538 | | 100 |

Using (1), the $S/N$ ratio values were computed for deposition rate, water contact angle, and MB absorbance in the $TiO_2$ compact layers coatings, as shown in Table 2. The hydrophilicity of the $TiO_2$ films was determined by measuring the water contact angle. The change in the water contact angle is shown as a function of UV irradiation time for the $TiO_2$ films deposited with parameter sets in the orthogonal arrays (Table 2). When the $TiO_2$ film surface is irradiated by UV light for 12 min, the water contact angles of all of the films begin to decrease (less than 63°, sample number 9), which indicates that the film surface becomes more hydrophilic. The absorption spectra for the MB aqueous solution degraded by $TiO_2$ photocatalytic film after 240 min UV irradiation are shown for the orthogonal array settings (Table 2). The $TiO_2$ films deposited using the parameter sets in the orthogonal arrays from number 1 to number 9 show MB absorbance between 1.33 and 1.03.

An analysis of variance (ANOVA) was used to determine the effect of a change in the process parameters on the process response. Table 3 shows the ANOVA results for the deposition rate, the water contact angle, and the MB absorbance. Table 3 shows that the variables that most significantly affect the deposition rate, the water contact angle, and the MB absorbance are the rf power ($P$ = 84.45%, 33.68%, and 54.36%), the sputtering pressure ($P$ = 6.93%, 33.62%, and 14.07%), and the argon-oxygen ratio ($P$ = 7.00%, 28.56%, and 20.00%).

Grey relational analysis (GRA) provides an efficient solution to difficult problems that involve multiple performance characteristics that are uncertain, have multiple inputs, and generate discrete data. The objective of this study is to optimize the deposition parameters for the $TiO_2$ compact films using GRA, which is used extensively in various industries [16].

Table 4: The Grey relational grade and its ranking for the $TiO_2$ compact layer coatings.

| Exp. | Grey relational grade | Rank |
|---|---|---|
| 1 | 0.3595 | 8 |
| 2 | 0.3526 | 9 |
| 3 | 0.4252 | 6 |
| 4 | 0.4551 | 4 |
| 5 | 0.3914 | 7 |
| 6 | 0.4356 | 5 |
| 7 | 0.5698 | 3 |
| 8 | 0.7007 | 2 |
| 9 | 0.8329 | 1 |

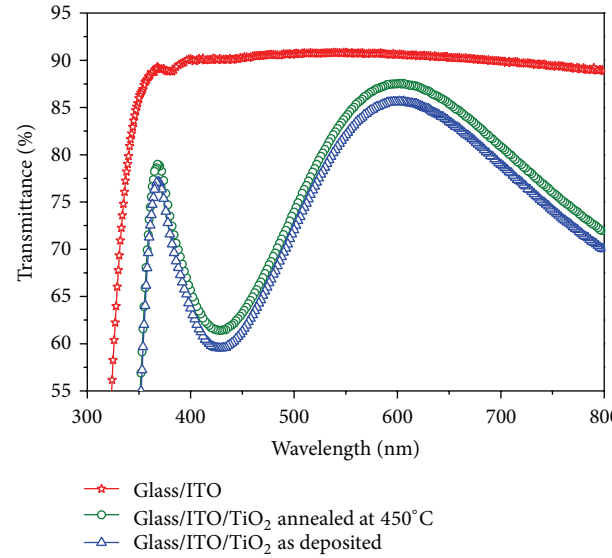


Figure 2: The optical transmittance spectra for $TiO_2$ compact layer/ITO/glass.

The optimum combination does not yield suitable process parameters with a single performance characteristic (Taguchi method) for the $TiO_2$ compact films coated. In order to optimize the deposition parameters, the deposition rate, the contact angle, and the MB absorbance, multiple performance characteristics (grey relational analysis) must be analyzed. The calculated grey relational grade is taken as the inspected value in the Taguchi method. Table 4 shows the grey relational grade and its ranking for the $TiO_2$ compact layer coatings. A comparison of the experimental results for the orthogonal array ($A_3B_3C_2D_1$) and the photocatalytic activity optimal parameter set ($A_3B_3C_2D_3$) for $TiO_2$ film deposition is shown in Table 5. The multiple performance characteristics for the deposition of $TiO_2$ thin films are greatly improved

Table 5: The confirmation test results for the multiple performance characteristics, using the initial and the optimal process parameters.

| Level | Initial process parameters $A_3B_3C_2D_1$ | Optimal process parameters $A_3B_3C_2D_3$ | Improvement rate (%) |
|---|---|---|---|
| Deposition rate (Å/min) | 4.775 | 5.48 | 12.87 |
| Contact angle (degree) | 63.09 | 53.47 | 15.25 |
| MB absorbance | 1.0305 | 0.865 | 16.06 |

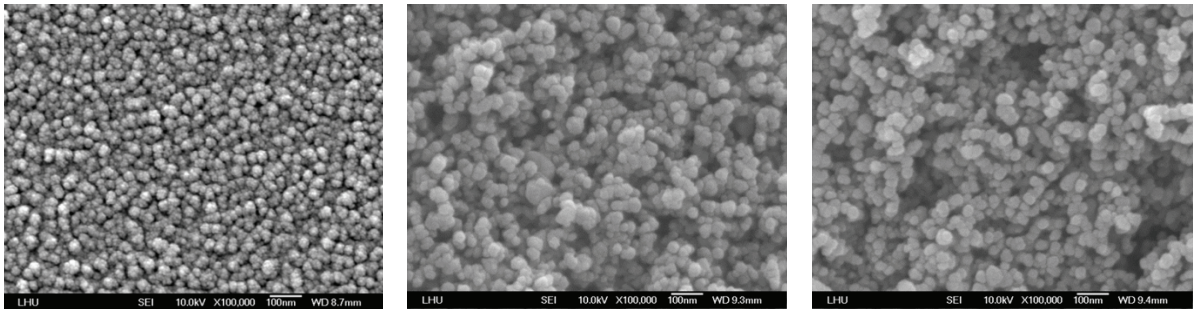


(a) (b) (c)

Figure 3: (a) The SEM images for sputtered $TiO_2$ compact layer on ITO/glass, (b) the SEM images for porous $TiO_2$ onto $TiO_2$ compact/ITO/glass, produced using the sol-gel with spin coating method, and (c) the SEM images for porous $TiO_2$ onto $TiO_2$ compact/ITO/glass, produced using the sol-gel with blade coating method.

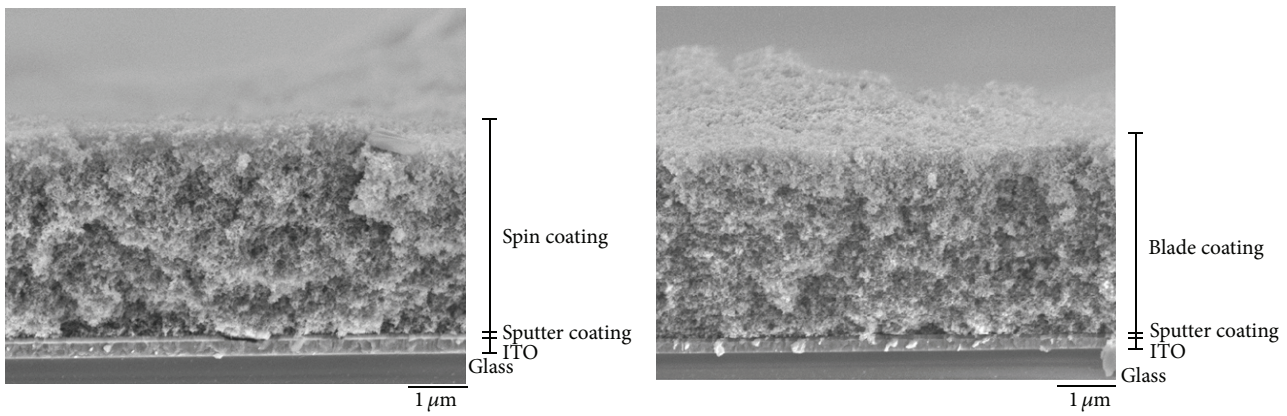


(a) (b)

Figure 4: The SEM cross-sectional image of $TiO_2$ (a) corresponding to Figure 3(b) and (b) corresponding to Figure 3(c).

Table 6: The performance of a DSSC prepared using a photoelectrode with and without a $TiO_2$ compact layer, using carbon and Pt counter electrodes, and using ITO/glass and FTO/glass.

| | $V_{oc}$ (V) | $J_{sc}$ (mA/cm$^2$) | Fill factor | Efficiency $\eta$ (%) |
|---|---|---|---|---|
| ITO/sputter/spin coating/carbon | 0.54 | 4.38 | 0.676 | 1.59 |
| ITO/sputter/blade coating/carbon | 0.53 | 4.08 | 0.666 | 1.44 |
| ITO/spin coating/carbon | 0.52 | 3.18 | 0.639 | 1.05 |
| ITO/blade coating/carbon | 0.52 | 3.07 | 0.572 | 0.90 |
| ITO/sputter/spin coating/Pt | 0.51 | 12.86 | 0.678 | 4.46 |
| ITO/sputter/blade coating/Pt | 0.49 | 10.73 | 0.675 | 3.51 |
| ITO/spin coating/Pt | 0.58 | 6.02 | 0.644 | 2.24 |
| ITO/blade coating/Pt | 0.61 | 5.10 | 0.649 | 2.01 |
| FTO/sputter/spin coating/Pt | 0.70 | 17.22 | 0.641 | 7.73 |
| FTO/sputter/blade coating/Pt | 0.77 | 12.79 | 0.750 | 7.36 |
| FTO/spin coating/Pt | 0.79 | 12.39 | 0.692 | 6.79 |
| FTO/blade coating/Pt | 0.79 | 10.80 | 0.771 | 6.53 |

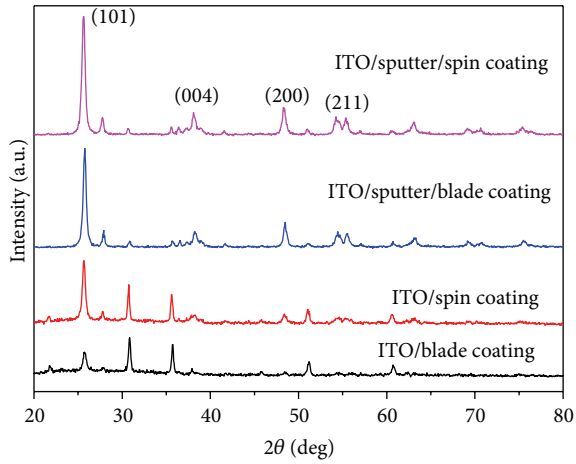


FIGURE 5: The XRD patterns for the $TiO_2$ films after being annealed at 450°C.

by using the Grey-Taguchi method. The improvement in the deposition rate is 12.87%, that in the water contact angle is 15.25%, and that in the MB absorbance is 16.06%.

The transmittance spectra are shown as a function of wavelengths in the range between 300 and 800 nm for $TiO_2$ compact layers in Figure 2. The average transmittance in the visible region exceeds 85% for all samples, but transmission in the UV-near visible region decreases abruptly. After annealing treatment, the optical transmittance of the film is increased.

*3.2. DSSC Conversion Efficiency.* SEM analysis was used to determine the morphology of the sputtered $TiO_2$ compact layers (with photocatalytic activity optimal parameters, $A_3B_3C_2D_3$) on the ITO substrate and the thick $TiO_2$ porous layer produced using the sol-gel method, as shown in Figure 3. The uniform and smooth surfaces of the sputtered compact accumulation film are well covered by spherical particles, which are densely coated with a small grain size (Figure 3(a), $TiO_2$ compact/ITO/glass). This is necessary to prevent charge recombination between the ITO and the porous $TiO_2$ layer [17, 18]. The SEM images show the porous $TiO_2$ film over the sputtered compact layer, produced using the sol-gel with spin coating method (Figure 3(b), porous $TiO_2$/$TiO_2$ compact/ITO/glass) and the sol-gel with blade coating method (Figure 3(c), porous $TiO_2$/$TiO_2$ compact/ITO/glass). The porous $TiO_2$ film structure is not dense and the crystallite size of the $TiO_2$ is increased. DSSC efficiency is improved by producing a $TiO_2$ electrode with a large surface area and optimum pore structure [19, 20].

The cross-section of the $TiO_2$ films was observed by SEM. Figure 4(a) corresponds to Figure 3(b) and Figure 4(b) corresponds to Figure 3(c). The $TiO_2$ compact/ITO films produced using the photocatalytic activity optimal deposition conditions ($A_3B_3C_2D_3$) are highly compacted and homogeneous and adhere perfectly to the glass substrate. These results confirm a spongelike structure for the $TiO_2$ layer (Figure 4), which is a prerequisite for a highly efficient DSSC [21]. The characteristics of the $TiO_2$ materials depend significantly upon the surface morphology, the crystal structure, and the crystallization.

Figure 5 shows that the XRD patterns of the $TiO_2$ films, produced using the sol-gel with spin coating of porous $TiO_2$/$TiO_2$ compact/ITO/glass, show a good crystalline structure and anatase (101) diffraction peaks that demonstrate a higher crystallinity than the other films. In contrast, without the $TiO_2$ compact layer (only porous $TiO_2$), the peak intensity of the anatase (101) plane in the XRD patterns for the $TiO_2$ film has a lower value, which demonstrates inferior crystalline quality.

Good performance for the counter electrode requires a low internal resistance and raw material cost. The best material for the counter electrode is Pt, which shows excellent electrochemical activity for $I_3^-$ reduction at film thicknesses of 2~10 nm [22, 23]. Figure 6 shows the photo current-voltage ($I$-$V$) characteristics for the DSSC under AM1.5 solar irradiation with 100 mW/cm$^2$ illumination, with and without the $TiO_2$ compact layer. Figure 6(a) shows a carbon counter electrode and ITO/glass, Figure 6(b) shows a Pt counter electrode and ITO/glass, and Figure 6(c) shows a Pt counter electrode and FTO/glass [24]. The corresponding cell parameters are summarized in Table 6, which shows the performance of the DSSC. With a $TiO_2$ compact layer to prevent charge recombination, a higher $J_{sc}$ is obtained. The energy conversion efficiency ($\eta$) increases if a Pt counter electrode is used instead of a carbon counter electrode.

For the purposes of comparison, the energy conversion efficiency for the DSSC film deposited on FTO glass is also given. FTO substrates have good optoelectronic performance and higher energy conversion efficiency than ITO substrates. Table 6 shows that a FTO/sputter/spin coating/PT setup increases the conversion efficiency of the DSSC, with $V_{oc}$ = 0.70 V, $J_{sc}$ = 17.22 mA/cm$^2$, a fill factor = 0.641, and an energy conversion efficiency as high as 7.73%.

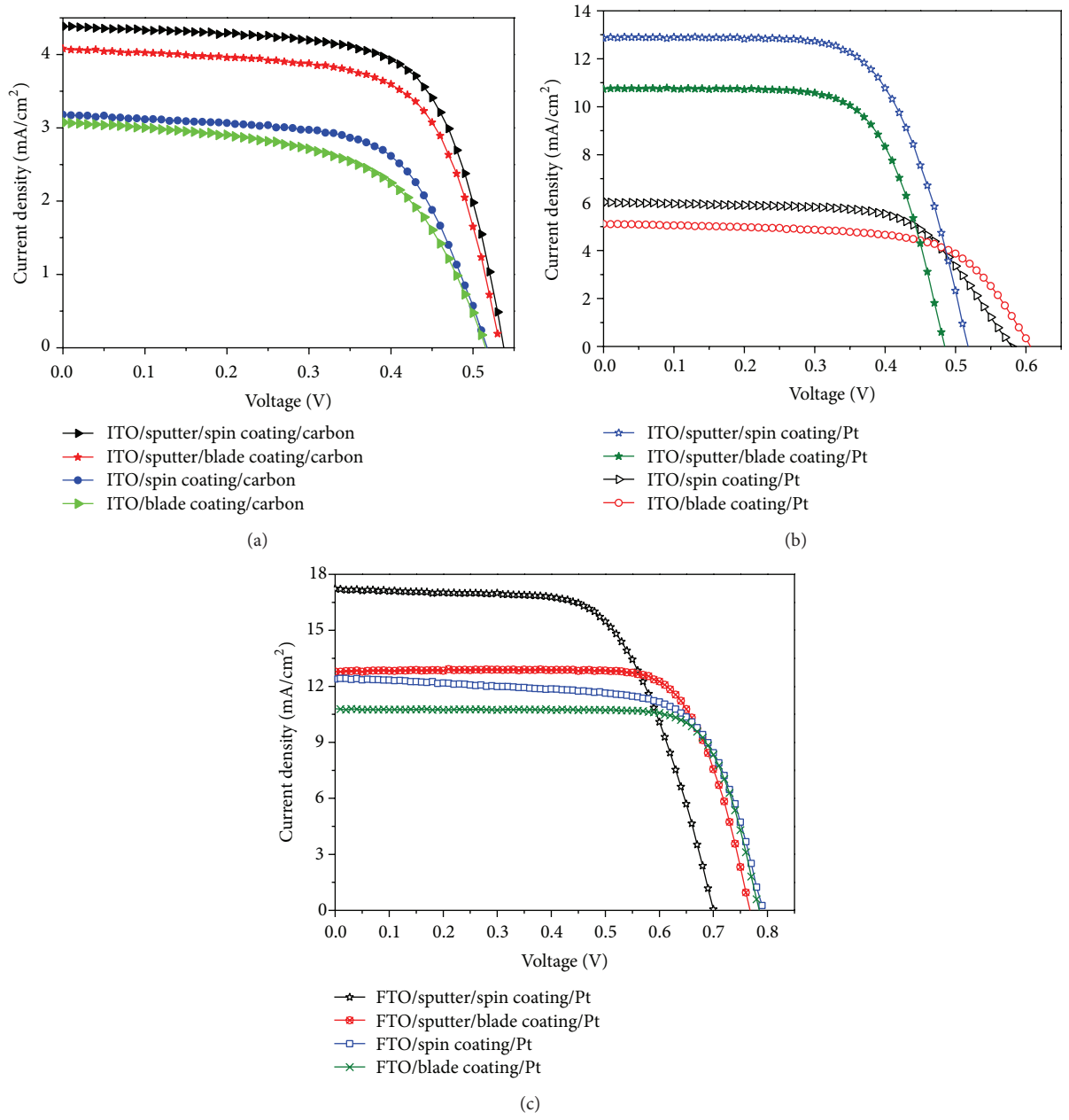


FIGURE 6: The *I-V* characteristics for DSSCs fabricated with and without a $TiO_2$ compact layer, (a) using a carbon counter electrode and ITO/glass, (b) using a Pt counter electrode and ITO/glass, and (c) using a Pt counter electrode and FTO/glass, under AM 1.5 solar irradiation with a density of 100 mW/cm$^2$.

## 4. Conclusion

$TiO_2$ films (compact layer) are coated onto ITO/glass substrates (and FTO/glass), using rf magnetron sputtering. The reactive and sputtering gases are $O_2$ and Ar, respectively. The multiple performance characteristics for the deposited $TiO_2$ compact films' photocatalytic activity are greatly improved by using the Grey-Taguchi method. The improvement in the deposition rate is 12.87%, that in the water contact angle is 15.25%, and that in the MB absorbance is 16.06%. The porous $TiO_2$ film that covers the sputtered compact layer produced by the sol-gel method has a structure which is not dense and a crystallite size that is increased. The XRD patterns for $TiO_2$ films produced using sol-gel with spin coating of porous $TiO_2$/$TiO_2$ compact/ITO/glass result in a good crystalline structure and the anatase (101) diffraction peaks demonstrate a higher degree of crystallinity. The energy conversion efficiency ($\eta$) for a Pt counter electrode is greater than that for a carbon counter electrode. The experimental results show that FTO/sputter/spin coating/PT setup increases

the conversion efficiency of the DSSC, with $V_{oc}$ = 0.70 V, $J_{sc}$ = 17.22 mA/cm$^2$, the fill factor = 0.641, and an energy conversion efficiency as high as 7.73%.

## Conflict of Interests

The authors declare that there is no conflict of interests regarding the publication of this paper.

## Acknowledgments

The authors gratefully acknowledge the support of the Kung Chi Technology Co., Ltd., the Ministry of Education of Taiwan, through Grant nos. 102G-88-022 and 102 M-88-021, and the Chung-Shan Institute of Science & Technology (Armaments Bureau).

## References

[1] Y.-S. Jin, K.-H. Kim, W.-J. Kim, K.-U. Jang, and H.-W. Choi, "The effect of RF-sputtered $TiO_2$ passivating layer on the performance of dye sensitized solar cells," *Ceramics International*, vol. 38, no. 1, pp. S505–S509, 2012.

[2] K. Nithyanandam and R. Pitchumani, "Analysis and design of dye-sensitized solar cell," *Solar Energy*, vol. 86, no. 1, pp. 351–368, 2012.

[3] H. Chang, T. L. Chen, K. D. Huang, S. H. Chien, and K. C. Hung, "Fabrication of highly efficient flexible dye-sensitized solar cells," *Journal of Alloys and Compounds*, vol. 504, no. 1, pp. S435–S438, 2010.

[4] K. R. Bae, C. H. Ko, Y. Park et al., "Structure control of nanocrystalline $TiO_2$ for the dye-sensitized solar cell application," *Current Applied Physics*, vol. 10, no. 3, pp. S406–S409, 2010.

[5] C. G. Kuo, C. Y. Hsu, S. S. Wang, and D. C. Wen, "Photocatalytic characteristics of $TiO_2$ films deposited by magnetron sputtering on polycarbonate at room temperature," *Applied Surface Science*, vol. 258, pp. 6952–6957, 2012.

[6] C.-T. Wang and C.-F. Yen, "Titania nanocomposite thin films with enhanced photovoltaic efficiency: effects of Ti-alkoxide sol and compact layer," *Surface and Coatings Technology*, vol. 206, no. 8-9, pp. 2622–2627, 2012.

[7] M. C. Kao, H. Z. Chen, and S. L. Young, "Dye-sensitized solar cells with $TiO_2$ nanocrystalline films prepared by conventional and rapid thermal annealing processes," *Thin Solid Films*, vol. 519, no. 10, pp. 3268–3271, 2011.

[8] S. Yuan, Y. Li, Q. Zhang, and H. Wang, "Anatase $TiO_2$ sol as a low reactive precursor to form the photoanodes with compact films of dye-sensitized solar cells," *Electrochimica Acta*, vol. 79, pp. 182–188, 2012.

[9] J. Yu, Q. Li, and Z. Shu, "Dye-sensitized solar cells based on double-layered $TiO_2$ composite films and enhanced photovoltaic performance," *Electrochimica Acta*, vol. 56, no. 18, pp. 6293–6298, 2011.

[10] L. Meng, T. Ren, and C. Li, "The control of the diameter of the nanorods prepared by dc reactive magnetron sputtering and the applications for DSSC," *Applied Surface Science*, vol. 256, no. 11, pp. 3676–3682, 2010.

[11] H. J. Kim, J. D. Jeon, D. Y. Kim, J. J. Lee, and S. Y. Kwak, "Improved performance of dye-sensitized solar cells with compact $TiO_2$ blocking layer prepared using low-temperature reactive ICP-assisted DC magnetron sputtering," *Journal of Industrial and Engineering Chemistry*, vol. 18, pp. 1807–1812, 2012.

[12] C.-C. Chen, C.-C. Tsao, Y.-C. Lin, and C.-Y. Hsu, "Optimization of the sputtering process parameters of GZO films using the Grey-Taguchi method," *Ceramics International*, vol. 36, no. 3, pp. 979–988, 2010.

[13] G. Taguchi, E. A. Elsayed, and T. Hsaing, *Quality Engineering in Production Systems*, McGraw-Hill, New York, NY, USA, 1989.

[14] P. C. Huang, C. H. Huang, M. Y. Lin, C. Y. Chou, C. Y. Hsu, and C. G. Kuo, "The effect of sputtering parameters on the film properties of molybdenum back contact for CIGS solar cells," *International Journal of Photoenergy*, vol. 2013, Article ID 390824, 8 pages, 2013.

[15] L. Zhang, Y. Zhu, Y. He, W. Li, and H. Sun, "Preparation and performances of mesoporous $TiO_2$ film photocatalyst supported on stainless steel," *Applied Catalysis B: Environmental*, vol. 40, no. 4, pp. 287–292, 2003.

[16] J. L. Deng, *The Essential Method of Grey Systems*, HUST Press, Wuhan, China, 1992.

[17] S. Vijayalakshmy and B. Subramanian, "Enhanced performance of dye-sensitized solar cells with $TiO_2$ blocking layers and Pt counter electrodes prepared by physical vapor deposition (PVD)," *Electrochimica Acta*, vol. 116, pp. 334–342, 2014.

[18] C. G. Kuo, C. F. Yang, L. R. Hwang, and J. S. Huang, "Effects of titanium oxide nanotube arrays with different lengths on the characteristics of dye-sensitized solar cells," *International Journal of Photoenergy*, vol. 2013, Article ID 650973, 6 pages, 2013.

[19] K. H. Ko, Y. C. Lee, and Y. J. Jung, "Enhanced efficiency of dye-sensitized $TiO_2$ solar cells (DSSC) by doping of metal ions," *Journal of Colloid and Interface Science*, vol. 283, no. 2, pp. 482–487, 2005.

[20] C. G. Kuo, C. F. Yang, M. J. Kao et al., "An analysis and research on the transmission ratio of dye sensitized solar cell photoelectrodes by using different etching process," *International Journal of Photoenergy*, vol. 2013, Article ID 151973, 8 pages, 2013.

[21] M. Hocevar, U. O. Krasovec, M. Bokalic et al., "Sol-gel based $TiO_2$ paste applied in screen-printed dye-sensitized solar cells and modules," *Journal of Industrial and Engineering Chemistry*, vol. 19, pp. 1464–1469, 2013.

[22] C. H. Yoon, R. V. R. Vittal, J. Lee, W.-S. Chae, and K.-J. Kim, "Enhanced performance of a dye-sensitized solar cell with an electrodeposited-platinum counter electrode," *Electrochimica Acta*, vol. 53, no. 6, pp. 2890–2896, 2008.

[23] H. Chang, C. H. Chen, M. J. Kao, S. H. Chien, and C. Y. Chou, "Photoelectrode thin film of dye-sensitized solar cell fabricated by anodizing method and spin coating and electrochemical impedance properties of DSSC," *Applied Surface Science*, vol. 275, pp. 252–257, 2013.

[24] M. H. Abdullah and M. Rusop, "Multifunctional graded index $TiO_2$ compact layer for performance enhancement in dye sensitized solar cell," *Applied Surface Science*, vol. 284, pp. 278–284, 2013.